Conf-731101--33

THERMAL CONDUCTIVITY OF ORIENTED FIBROUS CARBON INSULATION FROM 300 TO 1300 K IN NITROGEN AND ARGON AT ONE ATMOSPHERE[a]

T. G. Godfrey and D. L. McElroy
Metals and Ceramics Division, Oak Ridge National Laboratory
Oak Ridge, Tennessee 37830

Z. L. Ardary
Development Division
Oak Ridge Y-12 Plant
Oak Ridge, Tennessee 37830

T. G. Godfrey
Metals and Ceramics Division
Oak Ridge National Laboratory
Oak Ridge, Tennessee 37830

24 pages
11 figures
2 tables

ABSTRACT

The thermal conductivity, λ, of three samples of oriented fibrous carbon insulation was measured from 300 to 1300 K in a radial heat flow apparatus. Preparation of the 0.18 g/cm^3 density samples by a vacuum filtration process from carbon fibers and powdered phenolic resin, characterization of the material after carbonization, and typical mechanical properties are presented.

The λ of these low-density composites depended on both the heat treatment temperature and the fiber orientation. For samples heat treated at 1575 K, the room-temperature λ perpendicular to the planes of fibers was about 0.5 mW $cm^{-1}K^{-1}$ and was three times as high in the direction parallel to the planes. At 1000 K, the λ in both directions had doubled, primarily because of the positive $d\lambda/dT$ of the amorphous carbon fibers. Material heat treated at 2775 K had a significantly higher room-temperature λ and a negative $d\lambda/dT$, indicating that a slight degree of ordering or graphitization had occurred in the fibers during heat treatment. At high temperatures, λ of all three samples increased markedly because of radiative heat transport.

INTRODUCTION

The extreme temperatures and severe radiation environment encountered in a fusion reactor place stringent requirements on thermal insulations. Of the many types of insulations available, one of a single component of relatively high purity would seem to be a logical candidate. Such a material has been developed at the Oak Ridge Y-12 Plant, primarily for use in advanced aerospace systems, and is based on carbon-bonded carbon fibers. Processing parameters as well as starting materials may be varied over wide ranges to produce simple or complex shapes of great diversity in properties. In the present paper, we review the development of the insulation material, present some typical mechanical properties, and discuss the temperature dependence of the thermal conductivity, λ, of three particular samples. The specimens had densities of about 0.18 g/cm^3 and were prepared such that directional effects in the well-oriented structures could be studied together with the effect of heat treatment temperature.

PREPARATION OF CARBON FIBER COMPOSITES

The fabrication process for the carbon-bonded carbon fiber composites is basically an extension of that developed by the Y-12 Plant for Palarite, a carbon-bonded silica fiber insulation with a temperature capability of about 1300 K in vacuum or inert atmospheres (1,2). The development of the carbon fiber composites and study of the effect of process and materials variables on thermal and mechanical properties have been reported elsewhere (3), so only a brief description will be presented here. These materials were developed to fill a need for a high-temperature, machinable, low-density

insulating solid whose properties could be tailored for specific applications. A flow diagram of the basic process is presented in Fig. 1.

Materials

Carbon Bond — The carbon-bond precursor was a B-stage phenolic resin molding powder[b] with a 7 μm average particle size and a 50 wt % carbon yield on pyrolysis. The present samples were prepared using 20 wt % resin to yield a low-density material containing about 11 wt % carbon as binder. For certain applications, the resin content might be greatly increased to optimize mechanical properties. In the development work referenced previously, the carbon-bond precursor was a reagent-grade potato starch that had a significantly lower carbon yield and also required a gelatinization step in the fabrication procedure.

Carbon Fibers — The precursor for the amorphous carbon fiber was Villwyte[c] rayon filament tow (bundle) with a nominal fiber diameter of 6 to 7 μm. Fibers with nominal length of 250 μm were obtained by precision chopping[d] with a flock cutter. The fibers were pyrolyzed with about 25 wt % carbon yield by heat treating at 1625 K in an inert atmosphere. The resulting carbon fibers were 5 to 6 μm in diameter and about 200 μm long. After pyrolysis, the fibers were vacuum-drawn through a Wiley mill[e] to separate fibers that were either naturally clumped or slightly bonded by the pyrolysis operation.

Slurry Preparation

A very dilute (<0.3 wt % solids) water slurry containing about four parts fibers to one part phenolic resin was thoroughly mixed by an agitator in a tank with an external pump in a loop to draw the slurry from the

bottom of the tank and return it to the top in order to counteract settling. This is shown schematically in Fig. 2.

Vacuum Molding Operation

A mandrel, typically made of perforated metal covered by a filter material such as paper, cloth, or felt, was used as the substrate for depositing the solids during filtration. The mandrel was placed in a molding container that was then filled with water. The slurry was pumped into the molding container at the same rate as water was drawn through the mandrel by vacuum. Agitation continued in the mixing tank until the slurry was exhausted and all solids were deposited on the mandrel. Vacuum filtration was continued until the molding dewatered to a solids-to-water ratio of about 1.

Drying, Curing, and Carbonizing

The molding was heated to about 400 K on the mandrel in a drying oven to remove the water and simultaneously fuse the phenolic resin. The resulting shape was sufficiently rigid that it could be removed from the mandrel and handled without distorting. Because of the skeletal network of the carbon fibers, shrinkage during drying was insignificant.

The resin was pyrolyzed to effect the carbon bond by heating in an inert atmosphere to 1275 K or greater. The present samples were heated to 1575 and 2775 K to study the effect of heat treatment on the insulation thermal conductivity.

CHARACTERIZATION AND PROPERTIES

During the development of fibrous carbon insulations, many parametric studies were made of the relationships between batch proportions, fiber

lengths and diameters, and curing and furnacing steps, and the resulting density, strength, and thermal conductivity. As mentioned previously, potato starch was the carbon-bond precursor initially, and most property information was obtained on samples made with it (3). There has been no indication, however, that the substitution of the phenolic resin for starch significantly affects properties on an equivalent-carbon basis.

Microstructure

The oriented character of this fibrous insulation is evident in the scanning electron microscope (SEM) photographs of Fig. 3. The vast majority of the fibers are parallel to the mandrel surface and are cross linked at relatively few points. The fibers are well distributed in space with very little clumping. The nature of a typical fiber-to-fiber bond, as shown in the SEM of Fig. 4(a), is a web-like membrane, the thinness of which is clearly indicated by the transmission electron micrograph of Fig. 4(b).

Mechanical Properties

The mechanical properties of fibrous carbon insulations may be varied over a wide range, principally by control of fiber population (density) and binder content. For example, increasing fiber population to yield density levels of 0.35 and 0.6 g/cm^3 produces composites having, respectively, 600 and 2000 psi compressive strengths at 10% strain. The earlier studies (3) showed generally that factors that increased strength resulted in moderate increases in thermal conductivity. A 100% increase in compressive strength will typically increase λ by about 10%.

Typical flexural strength properties are shown in Fig. 5 as a function of binder content. For the range of binder content shown, the bulk density varies from about 0.11 to 0.20 g/cm^3. The compressive behavior of the

insulation material in the direction perpendicular to the fiber array is shown in Fig. 6 (4). Essentially elastic strain occurs up to 40 psi and 3% strain, after which structural degradation occurs. After continued strain to 10%, the material recovers on unloading to its starting geometry, but due to the degradation, it has a lower modulus. Repeated loadings to 10% strain show the resilient character of the material.

Irradiation Behavior (5)

An irradiation program as such has not been undertaken to evaluate the performance of fibrous carbon insulation. However, an end-cap insulator 1.02 cm o.d. by 1.02 cm long made from material heat treated at 2775 K was irradiated in the High Flux Isotope Reactor (HFIR) for 4 cycles at 100 MW at a thermal flux (<0.18 MeV) of 1.61×10^{15} n cm^{-2} sec^{-1} to thermal fluence of 1.18×10^{22} n/cm^2 (fast fluence of 3.75×10^{21} n/cm^2). The hot face temperature was calculated to be 1130 K and the cold face, 570 K. Precise diameter measurements were difficult to obtain because of the resilient nature of the material, but indications were that the linear shrinkage was less than 5%. There was no evidence of decrepitation of the piece.

RADIAL HEAT FLOW APPARATUS

The radial heat flow apparatus employed for thermal conductivity measurements on the insulating carbon was originally designed for samples of moderate to high conductivity ($20 < \lambda < 2000$ mW cm^{-1} K^{-1}) and has been described in detail elsewhere (6). The basic features of the apparatus are shown in Fig. 7. The radial temperature gradient in the 7.6-cm-diam by 22.8-cm-tall sample is produced by the axial core heater powered by a regulated, stable dc power supply. The dissipated $E \cdot I$ is determined potentiometrically from the voltage drop across the central section of

the heater and that across a 0.01-Ω standard resistor in series with the core heater and dc power supply. The overall temperature of the system is dictated by the three-section, noninductively wound muffle heater, each section being independently controlled. End guard pancake heaters are used to minimize axial heat flow in the sample. The temperature distribution within the sample is determined by 16 reference-grade 0.25-mm-diam Pt—10% Rh vs Pt thermocouples in high-purity twin-bore alumina insulators. The thermocouples enter the specimen disks radially and then turn 90° to assume an axial orientation that is presumably isothermal. The depth of immersion in the isothermal region is 30 times the wire diameter, which we judge to be sufficient to prevent errors due to heat leak along the thermocouple. Six thermocouples, three each at an inner radius and three each at an outer radius, are located in each of two measuring disks at the center of the sample stack for the primary determination of the radial temperature gradient. The extreme top and bottom disks are each provided with two thermocouples at the same radii as in the measuring disks for determination of the axial temperature profile of the stack. The thermocouple reference junctions to high purity copper wire are maintained at the ice point, and all wire, solder, and switches are of the low thermal emf type. Emfs are determined by use of a 6-dial Rubicon potentiometer[f]. Conversion of emf to temperature on IPTS-68 was by spline-fitted polynomials from Adams and Simpson (7).

The thermal conductivity was determined by

$$\lambda = \frac{q \ln r_2/r_1}{2\pi(\Delta T_{data} - \Delta T_{ISO})} ,$$

where

q = joule heat dissipated per unit length by the core heater,

r_2 = radius at outer thermocouple,

r_1 = radius at inner thermocouple,

ΔT_{data} = average temperature difference between the twc radii when core heater is powered, and

ΔT_{ISO} = isothermal correction.

The isothermal correction was obtained with zero power to the core heater, and the various heaters were adjusted to yield the same average specimen temperature as for the data mode. Its function is to provide an in-situ intercomparison of the thermocouples, and its importance has been described in detail elsewhere (6).

The absolute accuracy of results obtained with the radial heat flow apparatus is very difficult to assess, especially in the present case of very low-λ samples. Analysis of determinate errors yields a most probable error of ±1.5% (6). The assessment of indeterminate errors, principally those discussed in the following section, is not straightforward. Our "best guess" is about ±3.5%, which yields a maximum probable error of ±5%.

TEMPERATURE DISTRIBUTION CALCULATIONS

Because the present radial heat flow apparatus was developed for materials of moderate to high λ, the current studies made it necessary to establish its capabilities on very poor conductors ($\lambda < 4$ mW cm^{-1} K^{-1}). Even very slight temperature gradients on components in the apparatus could represent significant extraneous heat flows during measurements on insulators where the total heat flow is small. Experimental testing to assess these extraneous heat flows is slow and tedious in the apparatus. Therefore, a

finite difference steady-state and transient heat conduction code, HEATING-3 (8), was extensively employed to study the operating characteristics of the radial heat flow apparatus. These calculations were extremely valuable in aiding our interpretation of many experiments and have guided a program of improving the apparatus. The calculations performed were too detailed to present here, but some typical cases will be presented to illustrate the potential of this approach and the effects of various experimental details on the basic accuracy of the radial heat flow apparatus.

A section through an ideal radial heat flow apparatus is shown in Fig. 8, where all the heat generated by the axial core heater flows radially through the various concentric rings to the sink. Any real experimental apparatus can only approximate this mathematically infinitely long apparatus, and the extent to which the real apparatus accomplishes this is one aspect of its ultimate accuracy. In the present radial heat flow apparatus, as described in the previous section, the ends of the sample stack are guarded by flat disk heaters, and the surrounding muffle heater is in three sections to permit temperature profile adjustment. The apparatus is depicted in Fig. 9.

Calculations using HEATING-3 show that the temperature gradient on the core heater essentially reflects the temperature gradient on the muffle heater. If the muffle has a uniform heat generation rate, its ends are depressed in temperature to the extent that the core heater gradient yields an error of 10 to 15% in λ due to axial heat flow. This temperature distribution may be sensed by the thermocouples at the ends of the specimen stack, and the end guard heaters may be powered to reduce to end-to-center ΔT to zero. However, an hourglass profile would then occur, with the part of the specimen located between the end and center depressed in temperature.

This condition similarly leads to a heat leak from the central section of the core heater that may yield an error of 4 to 5% in λ.

Judicious juggling of the relative power inputs to the end and center sections of the muffle with simultaneous adjustments of the end guard heater power in the calculations can yield results that approximate the ideal case. However, this is very difficult to achieve experimentally because the number of thermocouples available is finite, and they must generally be placed in positions that are somewhat of a compromise. Even if the experimental system can be made to precisely duplicate the calculations of HEATING-3, the validity of results depends on the quality of the assumed property data for each component. This, of course, implies knowing the answer before the experiment is conducted. Nonetheless, parametric studies have been of significant benefit to the continuing development of the radial heat flow apparatus, particularly in the present instance of very low-λ samples, where the presence of small extraneous heat flows in core heater or sample may drastically affect the results.

THERMAL CONDUCTIVITY MEASUREMENTS

Description of Samples

The samples of insulating fibrous carbon for radial heat flow measurements were machined from heat-treated blanks that had been formed to yield two different fiber orientations. The first samples were made on a cylindrical mandrel so that the fibers were, in general, oriented with their long axes perpendicular to the heat flow direction. The orientation was sufficiently perfect that the appearance was one of onion-skin cylinders as shown in Fig. 10(a). One set of samples was heat treated in nitrogen at 1575 K (1575 $\perp$) and the other at 2775 K (2775 $\perp$). The other set of samples was

made on a flat mandrel so the fiber axes were parallel to the faces of the disks as shown in Fig. 10(b). Since the fibers assume all orientations within the planes of this mica-like structure, some do lie perpendicular to the heat flow direction, but the majority will have some radial component and are therefore considered to be parallel to the heat flow direction. This sample was also heat treated at 1575 K in nitrogen (1575 ||).

Bulk density of all samples was about 0.18 ± 0.01 g/cm^3 or approximately 0.10 volume fraction solids. Both 1575 samples and the 2775 K sample were amorphous according to x-ray diffraction.

Thermal Conductivity Results

Four assemblies of the apparatus were made for the three samples as described in Table I. The first assembly with the 1575 ⊥ sample employed a platinum-wound Al_2O_3 tube core heater, which proved to be a serious source of error, so a second assembly was made of this sample with a type 304 stainless steel tube core heater. These core heaters will be discussed later. Measurements on the 1575 || and 2775 ⊥ samples were made with the stainless steel core heater. All measurements were made at a gas pressure of 1 atm.

The results obtained for the three samples are shown in Fig. 11. For the 1575 ⊥ sample on first assembly, the measurements appeared to be satisfactory up to 800 K; but at the higher temperatures, the results were overly sensitive to small changes in temperature profiles within the specimen-heater components. Calculations using HEATING-3 confirmed that axial heat leaks from the core heater were the probable cause of the difficulty and that the end guard heaters were incapable of reducing the heat leak to an acceptable level without introducing other extraneous heat flows. An elaborate core heater was then constructed of 6.35-mm-diam,

0.5-mm-wall type 304 stainless steel tubing directly heated by the dc power supply. Independently adjustable platinum-wire heaters in twin-bore Al_2O_3 tubes were strapped to each end of the core heater just outside the specimen stack. Five Pt–10% Rh vs Pt thermocouples were spaced inside the core heater along its length and were thermally attached by wires welded in small radial holes in the tube wall. These permitted a measure of the temperature distribution over the length of the core heater. The axial thermal conductance at room temperature, relative to the sample, was 1.73 for the platinum-wound Al_2O_3 tube and 0.176 for the stainless steel tube. The additional heaters on the stainless steel tube in conjunction with the end guard heaters permitted near-zero axial heat flow to be obtained on all subsequent measurements. The results from the second assembly of the 1575 $\perp$ sample agreed well with the previous ones at lower temperatures and indicated a gradual increase in λ at the higher temperatures. Results on the 1575 $\parallel$ sample were similar to those of the 1575 $\perp$ sample but were about 3 times as high. Both sets of data were described well by expressions of the form

$$\lambda = a_0 + a_1 T^{1/2} + a_2 T + a_3 T^3 \text{ mW cm}^{-1} \text{ K}^{-1} ,$$

and these are shown as the solid lines through the results in Fig. 11. Coefficients for the two samples are given below.

Coefficients	1575 $\perp$	1575 $\parallel$
a_0	−0.88132	−4.42763
a_1	0.125895	0.51536
a_2	-2.6356×10^{-3}	-1.03482×10^{-2}
a_3	6.70872×10^{-10}	1.40685×10^{-9}

The results for the 2775 $\perp$ sample are totally different from those of the 1575 samples, and a functional fit of these data was not attempted. The negative temperature dependence of the lower temperature data for the 2775 K sample indicates that the sample was fundamentally different from the 1575 K samples. At the higher temperatures, the 2775 K sample results increase in λ, as do the other samples.

DISCUSSION OF RESULTS

The theory and measurement of heat transmission in fibrous materials has recently been reviewed by Pratt (9) and will not be repeated here. The effective conductivity of fibrous materials is obviously related to fiber conductivity; gas conductivity; the optical properties of the fiber; pore size, shape, and orientation; fiber size, shape, and orientation; bulk density; and gas pressure.

In view of the above, the present results were treated empirically with the expression

$$\lambda_m = x(\lambda_1 V_1 + \lambda_2 V_2) + y\left(\frac{\lambda_1 \lambda_2}{\lambda_1 V_2 + \lambda_2 V_1}\right),$$

proposed by Schuhmeister (10) for the conductivity, λ_m, of textile fabrics, where λ_1, λ_2 and V_1, V_2 denote the conductivity and fractional volume of gas and fiber, and $x + y = 1$. Schuhmeister assumed that $x = 1/3$ and $y = 2/3$ represented a weighted average of the series and parallel arrangements in a random mixture of fibers in fabric. Baxter (11) found empirically that values $x = 0.21$ and $y = 0.79$ gave better agreement for his measurements on several fabrics. Using Baxter's coefficients in the Schuhmeister expressions and recommended λ values for amorphous carbon and the gases from Ho et al. (12), the dashed lines in Fig. 11 were calculated for the 1575 $\perp$ sample.

For the 1575 || case, the x and y values were reversed, with the result also shown in Fig. 11. It should be noted that the Baxter-Schuhmeister expression is completely determined and is not forced to fit the present results. The experimental results are well described by the expression up to about 700 K for the 1575 ⊥ sample in argon and nitrogen, but only at the lowest temperature for the 1575 || sample. This expression should not be expected to describe the results over a wide temperature range since it considers heat conducted through the fibers and the gas but ignores radiation through the gas-filled voids. This is a valid assumption only at low temperatures for these very porous specimens. The slight upswing in the calculated conductivities reflects the increasing $d\lambda/dT$ in amorphous carbon at the higher temperatures.

Since the Baxter-Schuhmeister expression gave good agreement with the measurements on the 1575 ⊥ sample over a significant temperature range, it was used to calculate the λ of the fiber from the measured λ of the 2775 ⊥ sample for the three lowest temperature points of Fig. 11. The results are shown in Table 2 with the λ of amorphous carbon used in the previous calculations and recommended values from Ho et al. (12) for a typical graphite. The decreasing λ of the 2775 fiber with increasing temperature is taken as evidence that the 2775 treatment has initiated graphitization of the fibers, although the extent is too small for detection by routine x-ray diffraction.

The increasing divergence with temperature of the present results from the Baxter-Schuhmeister calculation is readily attributable to radiative heat transfer in the highly porous samples. The T^3 term in the equations that fit the results for both 1575 samples is necessary to describe the increasing slope at the higher temperatures, and such a term

is normally taken to indicate radiative heat transfer. Klemens and Greenberg (13) have analyzed radiative heat transfer through composite materials and have derived expressions relating photon mean free paths in fiber assemblies to geometrical factors. They find that the radiative heat transport varies in a complex fashion rather than in a simple T^3 manner and that extrapolation of the high-temperature T^3 relation will underestimate the radiation contribution to the total conductivity at lower temperatures. Evaluation of their expressions is not possible in the present case because of the limited temperature range of the data and because the expressions assume a random assembly of fibers rather than an oriented one. The greater divergence of the 1575 $\parallel$ results from the Baxter-Schuhmeister calculations compared with the 1575 $\perp$ results is possibly due to a difference in optical thickness of the two different fiber arrangements. The optical transmission of thin slices of both parallel and perpendicular specimens was determined with a Densichron[8], and significant differences were observed. For equivalent transmission, the parallel sample had to be 2 to 3 times as thick as the perpendicular sample and was opaque at about 0.5 mm thickness. The perpendicular sample was opaque at less than 0.25 mm thickness. Thus, the greater divergence of observed from calculated values for the 1575 $\parallel$ samples over that of the 1575 $\perp$ sample is readily explicable.

The 2775 $\perp$ results also indicate a large radiation contribution since the Baxter-Schuhmeister calculation would yield a conductivity that would continue to decrease with increasing temperature, if we assume that the lower temperature data indicates sufficient fiber graphitization to make $d\lambda/dT$ of the fiber negative, as is observed in graphite. Thus, the difference between the calculated and observed values must be attributed to radiative heat transport through the gas-filled voids.

CONCLUSIONS

A rigid, oriented fibrous carbon insulation has been developed to meet the needs of specific high-temperature applications, but this insulation has properties that make it attractive for many other uses. The material is of a single component, amorphous carbon, and may be processed to yield a wide range of property values. Compressive and flexural strengths are in the range of 100 and 500 psi, respectively, in low-density versions. Compressive strength is a function of density and may approach 10,000 psi in high-density composites. For material heat treated at 1575 K, the thermal conductivity increases with temperature and depends upon the fiber orientation. At room temperature in argon, λ is about 0.5 mW cm^{-1} K^{-1} in the direction perpendicular to the planes of fibers and about 1.4 mW cm^{-1} K^{-1} parallel to the planes. The λ of a specimen heat treated at 2775 K was about 2.7 mW cm^{-1} K^{-1} at room temperature and decreased with increasing temperature for several hundred degrees. This was taken to mean that the 2775 K heat treatment had initiated graphitization of the amorphous carbon.

The λ results of the 1575 K samples were well described at the lower temperatures by a mixture-type expression, but at higher temperatures radiative heat transfer caused a marked increase in the effective λ of these very porous insulators. The fiber orientation seemed to play an important role in radiative heat transfer, with the perpendicular sample being more opaque.

The Baxter-Schuhmeister equation describes the results so well over the lower temperature range that calculations of the λ of this material could be made for any gas in the void space.

ACKNOWLEDGMENTS

The authors would like to thank C. D. Reynolds and many other members of the Development Division of the Y-12 Plant for the fabrication and characterization of the insulation samples used in this work. We appreciate the helpful discussions with J. P. Moore, T. G. Kollie, and R. K. Williams during the conduct of the experiments and the preparation of this report.

REFERENCES

1. C. D. REYNOLDS and Z. L. ARDARY, "Palarite Thermal Insulation," Y-1716, Union Carbide Corporation, Nuclear Division, Oak Ridge Y-12 Plant (April 1970).

2. Z. L. ARDARY and D. H. STURGIS, "Rigidified Fibrous Silica Thermal Insulation," Y-1825, Union Carbide Corporation, Nuclear Division, Oak Ridge Y-12 Plant (February 1972).

3. Z. L. ARDARY and C. D. REYNOLDS, "Carbon Fiber Thermal Insulation," Y-1803, Union Carbide Corporation, Nuclear Division, Oak Ridge Y-12 Plant (March 1972).

4. L. G. RAINHART, Sandia Laboratory, Albuquerque, N.M., private communication.

5. B. H. MONTGOMERY, Oak Ridge National Laboratory, and C. B. POLLOCK, Oak Ridge Y-12 Plant, private communication.

6. T. G. GODFREY, W. FULKERSON, T. G. KOLLIE, J. P. MOORE, and D. L. McELROY, "Thermal Conductivity of Uranium Dioxide and Armco Iron by an Improved Radial Heat Flow Technique," ORNL-3556, Oak Ridge National Laboratory (June 1964).

7. R. K. ADAMS and R. L. SIMPSON, in *Temperature — Its Measurement and Control in Science and Industry*, Vol. 4, pp. 1457–1466, Instrument Society of America, Pittsburgh (1972).

8. W. D. TURNER and M. SIMON-TOV, "HEATING-3 — An IBM 360 Heat Conduction Program," ORNL-TM-3208, Oak Ridge National Laboratory (February 1971).

9. A. W. PRATT, in *Thermal Conductivity*, R. P. Tye, Ed., Vol. 1, pp. 301–405, Academic Press, New York (1969).

10. SCHUHMEISTER, *Ber. K. Akad. Wein*, 76, 283ff (1877) [cited by Pratt (9).]

11. S. BAXTER, "The Thermal Conductivity of Textiles," *Proc. Phys. Soc.*, 58, 105–18 (1946).

12. C. Y. HO, R. W. POWELL, and P. E. LILEY, "Thermal Conductivity of the Elements," Department of Commerce, National Bureau of Standards report (in press).

13. P. G. KLEMENS and I. N. GREENBERG, "Radiative Heat Transfer Through Composite Materials," *J. Appl. Phys.*, 44, 2992–95 (1973).

FOOTNOTES

a. Research sponsored by the U.S. Atomic Energy Commission under contract with the Union Carbide Corporation.

b. Durez 22352 Phenolic Resin, Product of Hooker Chemical Corporation, Durez Division, North Tonawanda, New York.

c. Product of Midland Ross, Inc., Cleveland, Ohio.

d. Performed by Micro-Fibers, Inc., Pawtucket, Rhode Island.

e. Product of Arthur H. Thomas Company, Philadelphia, Pennsylvania.

f. Minneapolis-Honeywell model 2768 Rubicon potentiometer, linearity ±0.01%, residual ±0.01 μV.

g. Product of W. M. Welch Scientific Company, Chicago, Illinois.

TABLE I.

Description of Assemblies of Insulating Carbon Samples in Radial Heat Flow Apparatus

Assembly	Sample	Core Heater	Temperature Range (K)	Atmosphere
1	1575 ⊥	Pt-Al_2O_3	300–600	Nitrogen
			600–1015	Argon
2	1575 ⊥	304 stainless steel	485–1075	Argon
3	1575 ∥	304 stainless steel	300–1275	Argon
4	2775 ⊥	304 stainless steel	300–1125	Argon

TABLE II.

Estimated λ of Carbon Fibers

Temperature (K)	Fiber Thermal Conductivity (mW cm^{-1} K^{-1})		
	1575 Sample[a]	2775 Sample[b]	39OS Graphite[c]
321	16.6	117.2	1770
470	20.1	112.0	1430
639	22.2	110.5	1145

[a]Values for amorphous carbon recommended in Ref. 12.

[b]Calculated from experimental data by the Baxter-Schuhmeister expression.

[c]Parallel to axis of extrusion. Values from Ref. 12.

LIST OF FIGURES

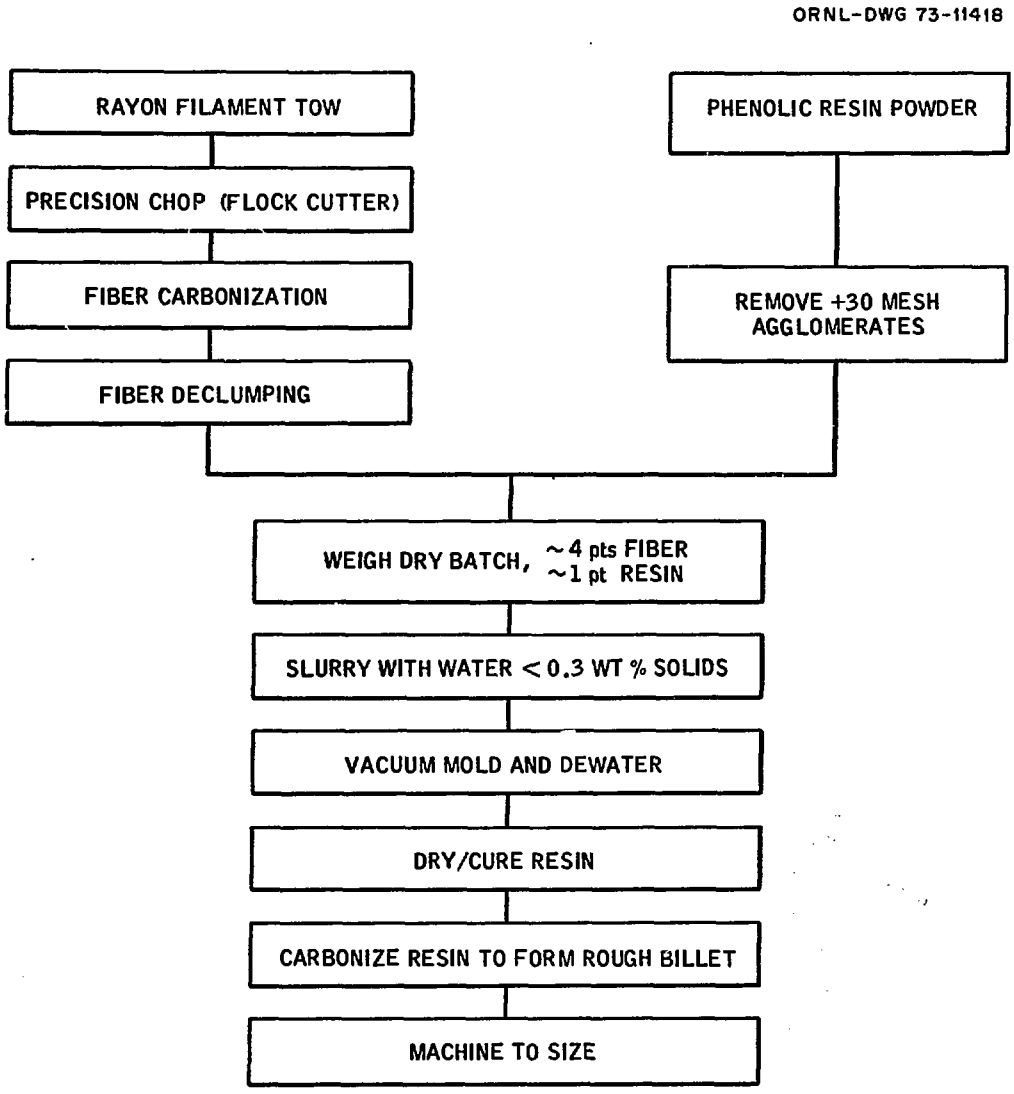

Fig. 1. Flow diagram for preparation of carbon-bonded carbon fiber insulation.

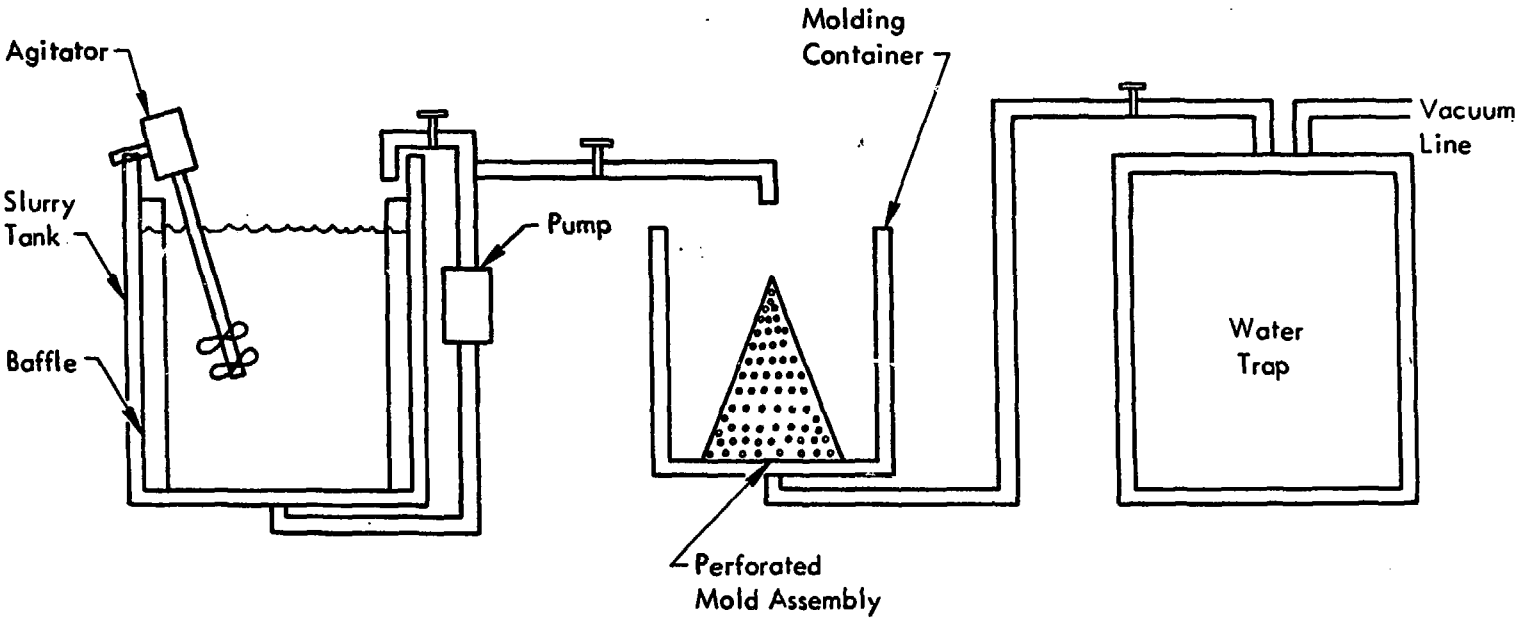

Fig. 2. Schematic diagram of equipment used to form fiber insulation.

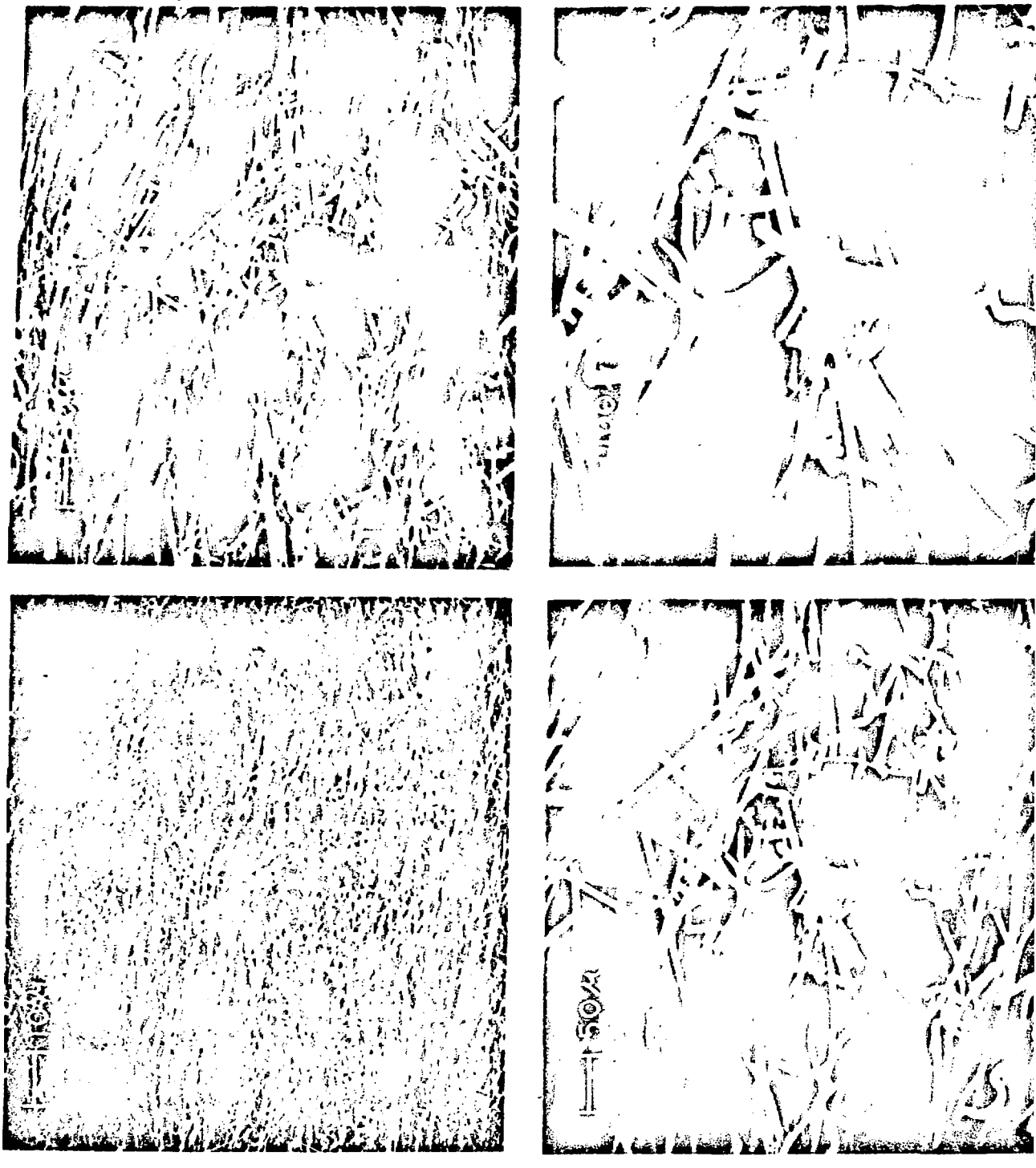

Fig. 3. Scanning electron microscope photographs of carbon-fiber composite.

Fig. 4. Details of the fiber-fiber carbon bond. (a) SEM photograph of the web-like bond between fibers (2140×). (b) Transmission electron micrograph showing the thinness of the carbon web (9000×).

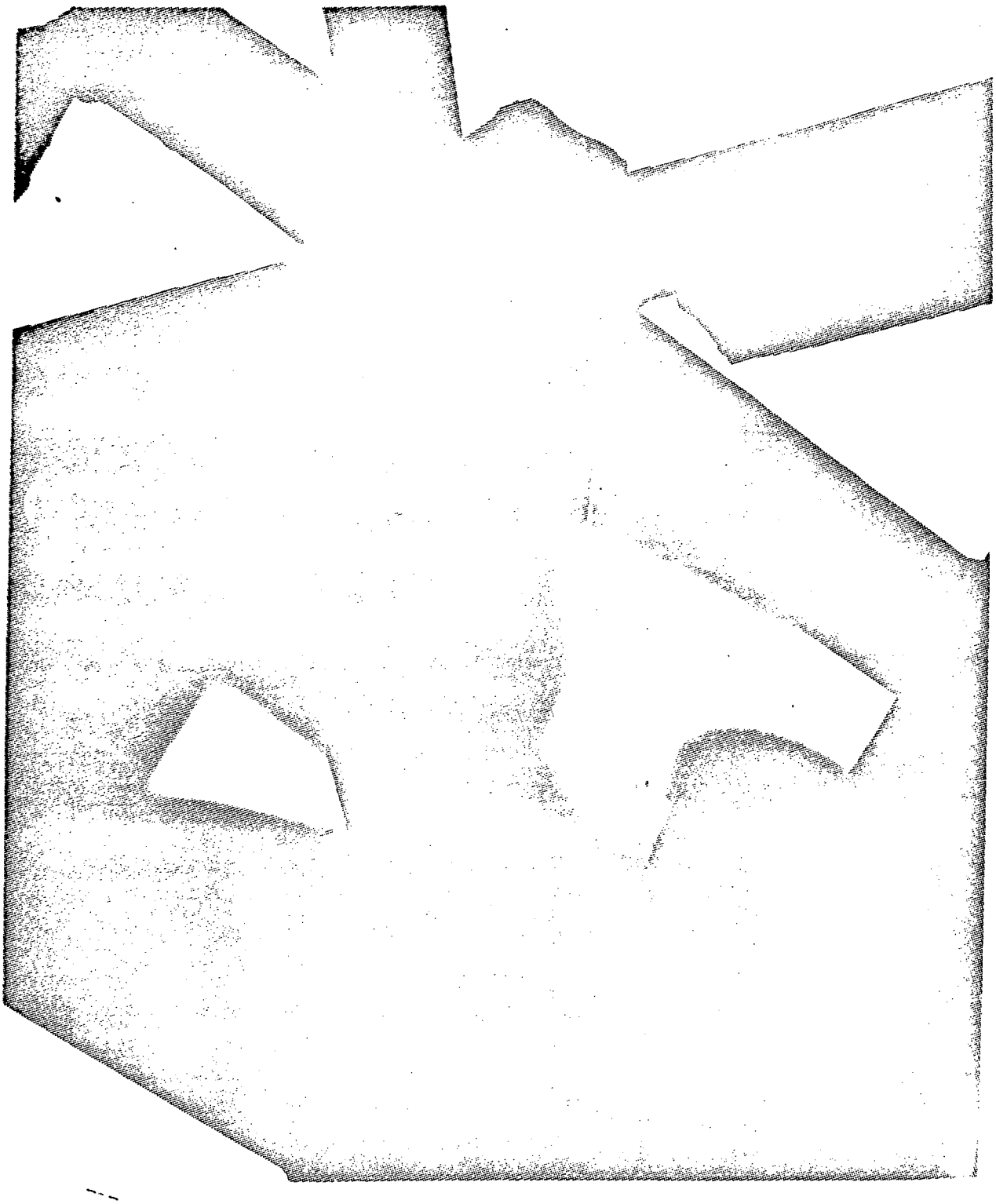

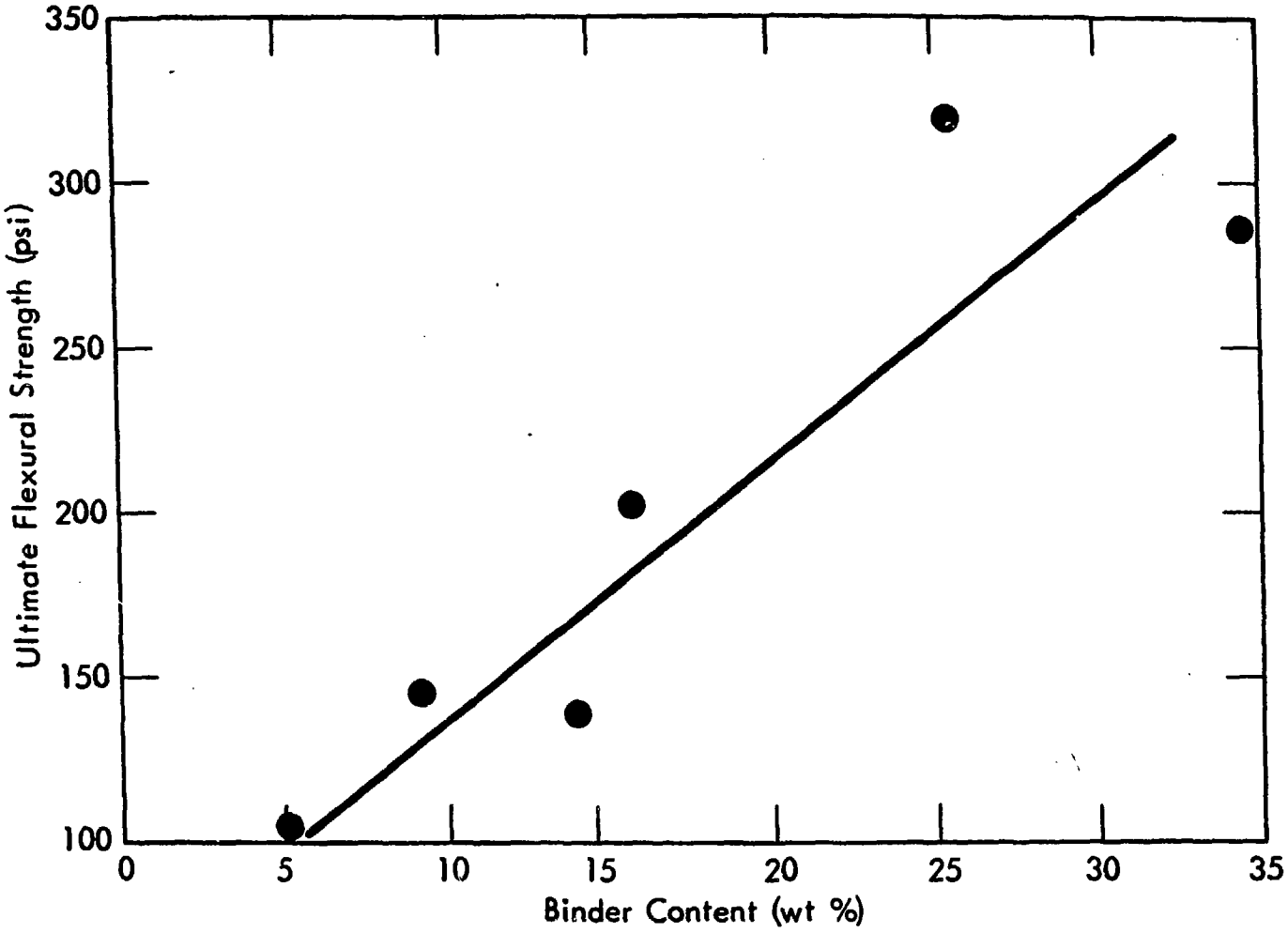

Fig. 5. Flexural strength as a function of carbon-binder content for carbon-fiber composites.

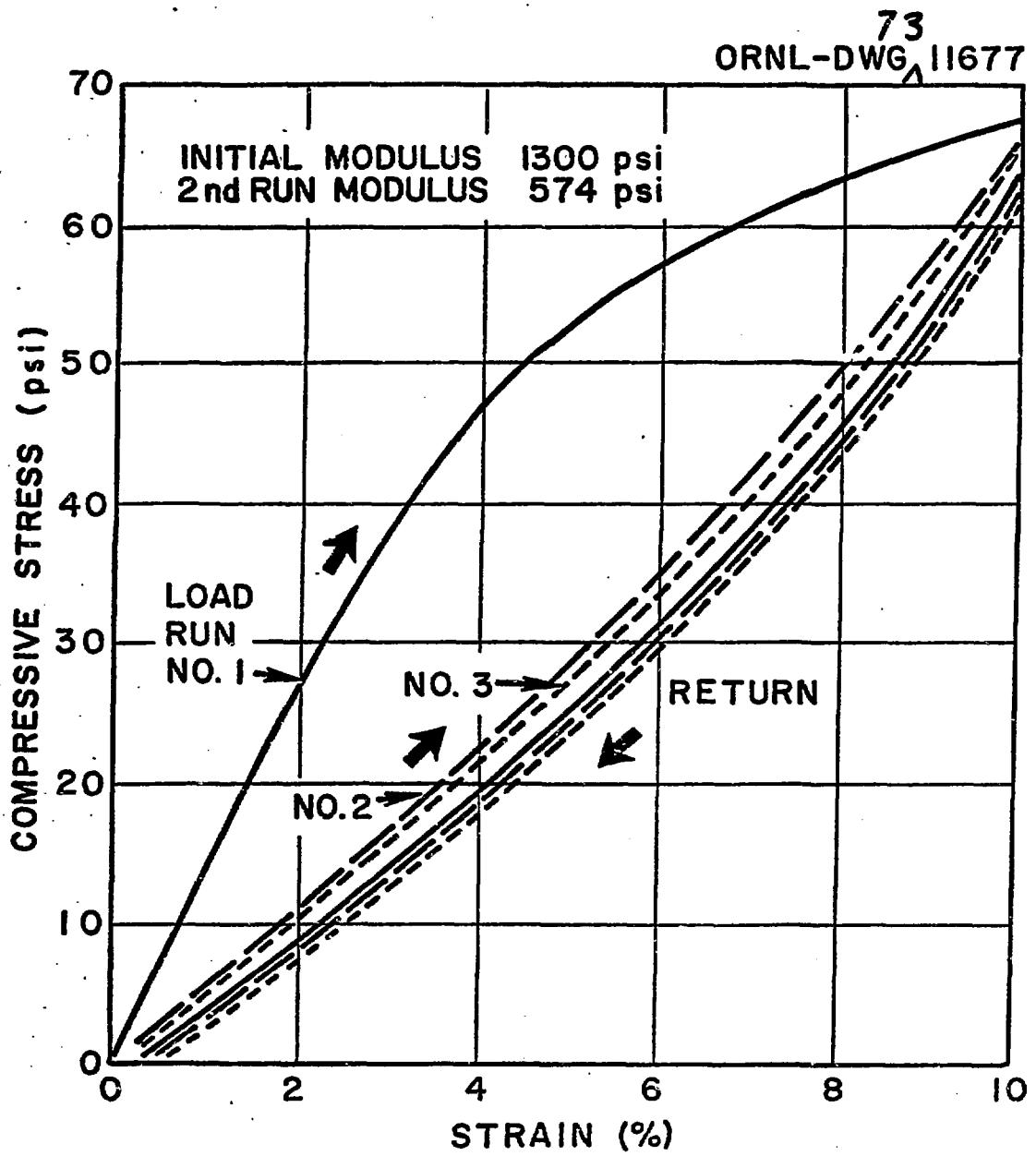

Fig. 6. Effect of repeated loading on carbon fiber insulation.

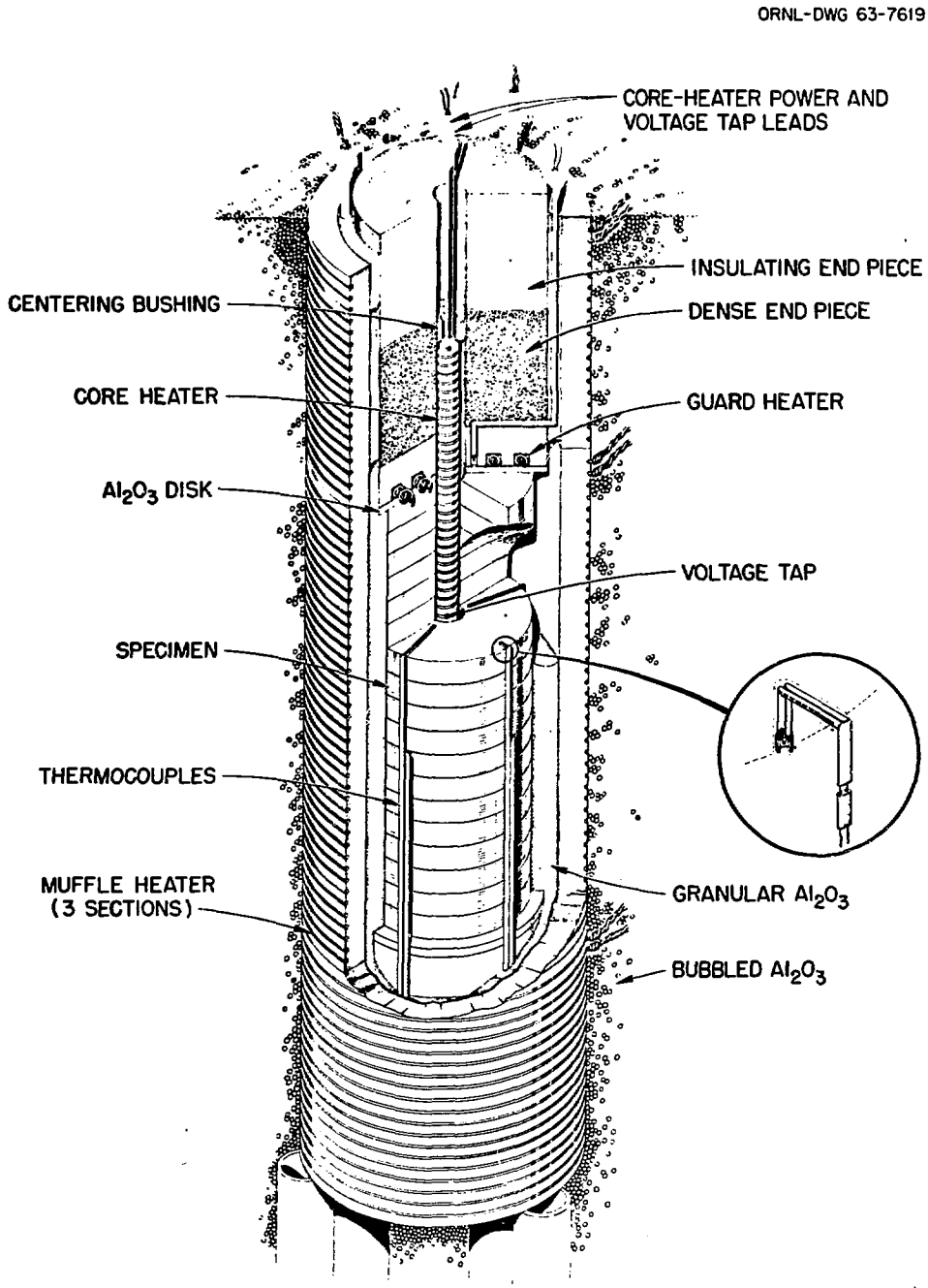

Fig. 7. The radial heat flow apparatus.

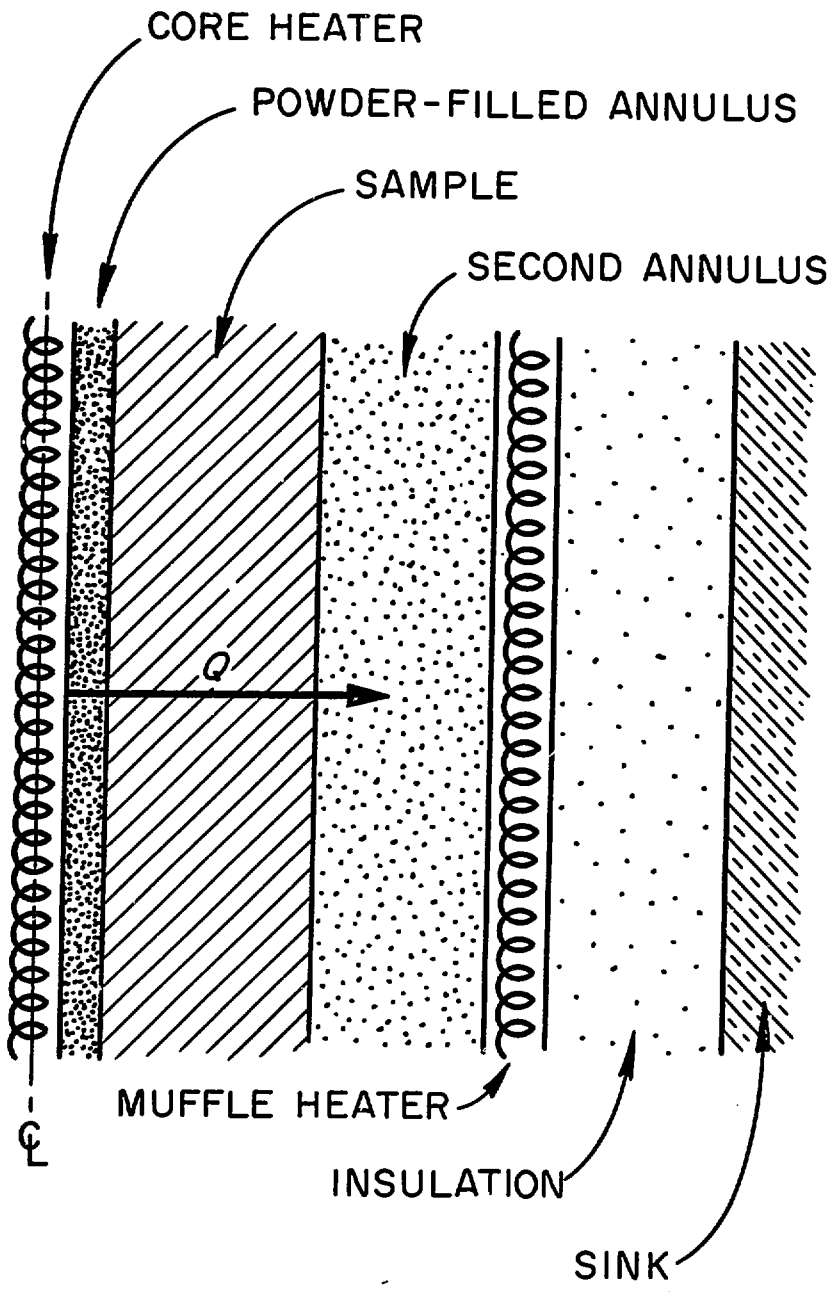

Fig. 8. Pictorial representation of an ideal radial heat flow apparatus that employs a surrounding muffle heater.

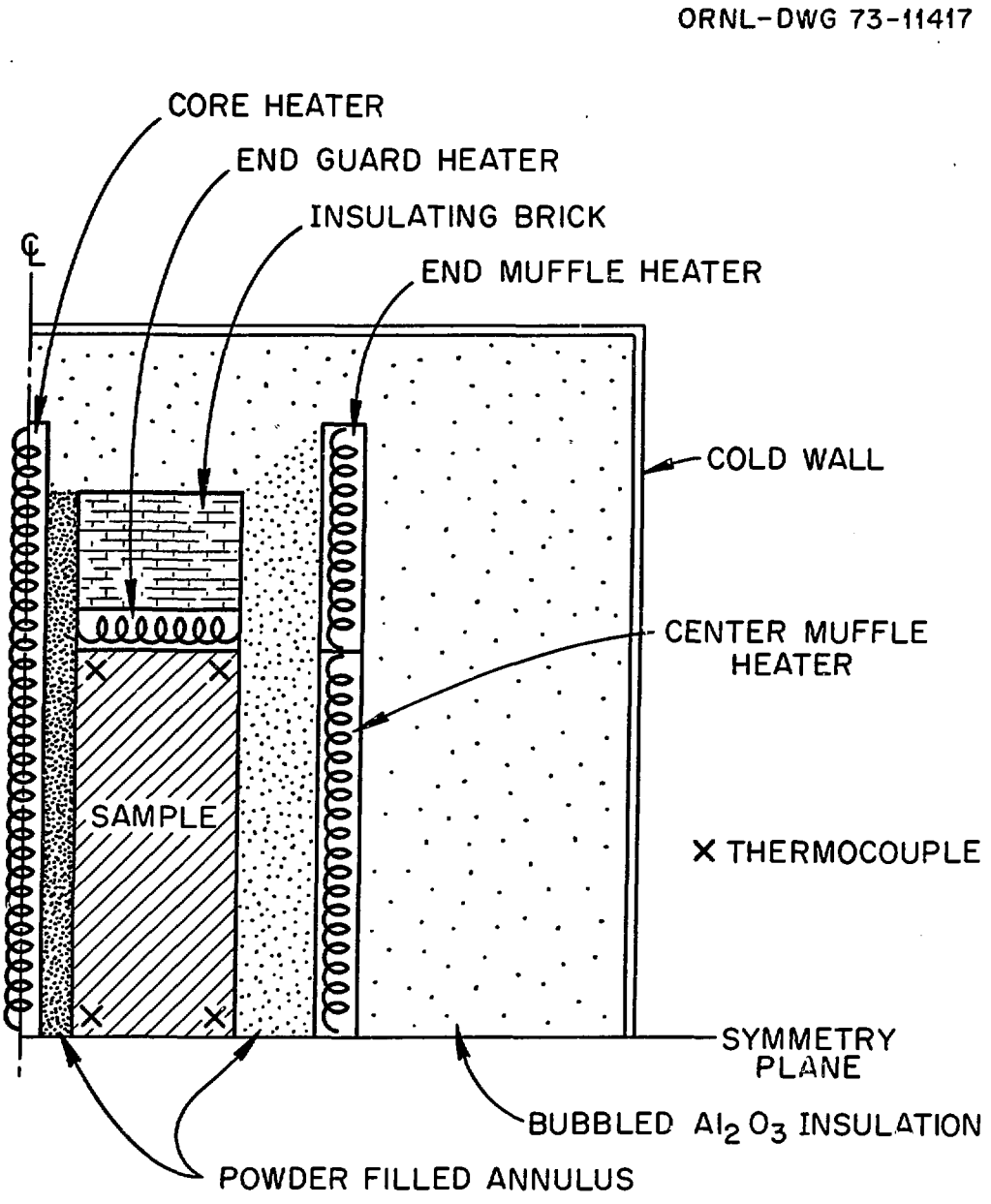

Fig. 9. Pictorial representation of the ORNL radial heat flow apparatus, showing the various heaters used to control axial and radial heat flow.

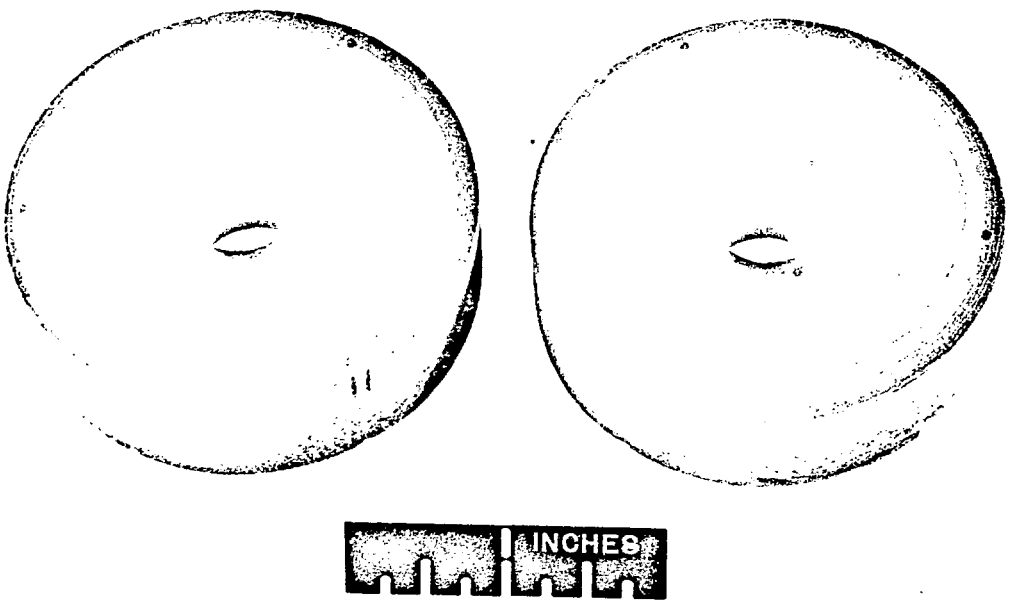

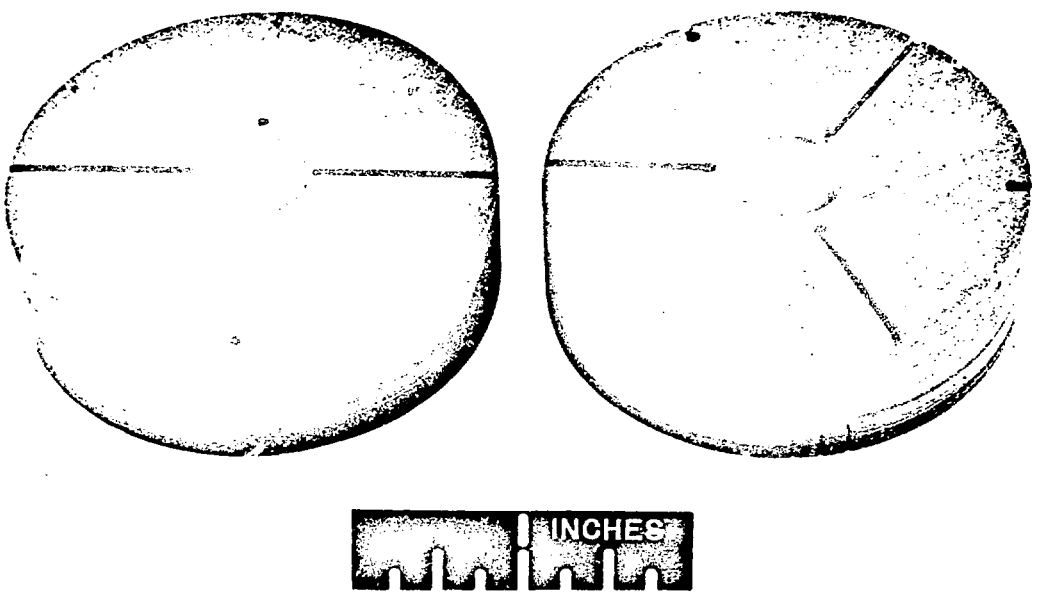

Fig. 10. Specimens of fibrous carbon used for thermal conductivity measurements. (a) Sample with fibers oriented perpendicular to heat flow direction (onion-skin cylinder). (b) Sample with fibers oriented parallel to heat flow direction (mica-like layers).

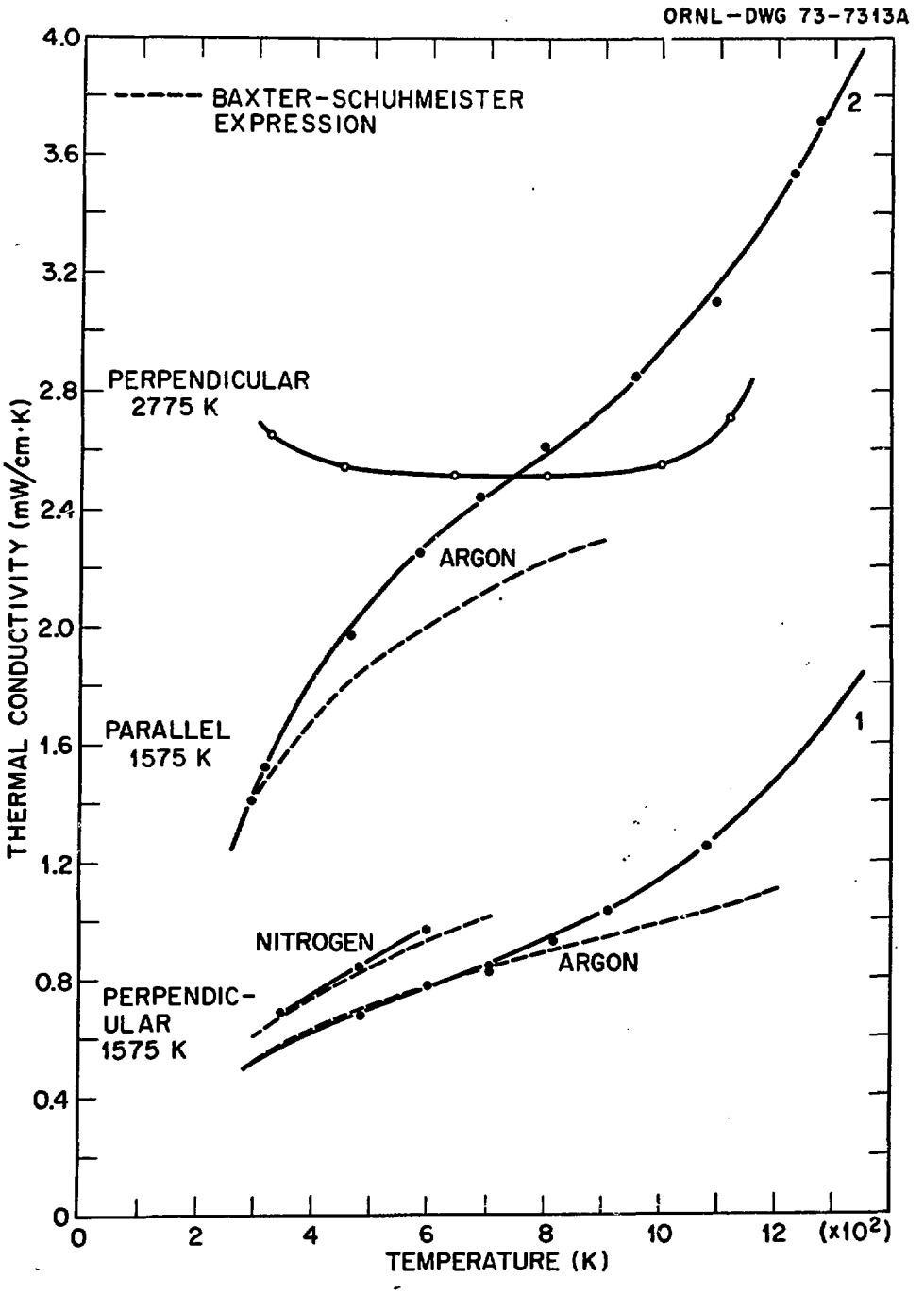

Fig. 11. Thermal conductivity of fibrous carbon insulation of two different orientations and two heat-treatment temperatures.